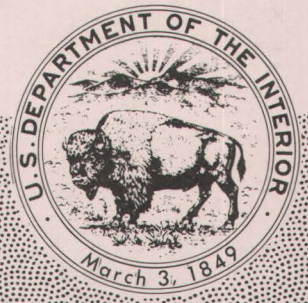


GEOLOGICAL SURVEY CIRCULAR 672



**Ground Motion Values  
for Use in the Seismic Design of the  
Trans-Alaska Pipeline System**



# **Ground Motion Values for Use in the Seismic Design of the Trans-Alaska Pipeline System**

**By Robert A. Page, David M. Boore,  
William B. Joyner, and Henry W. Coulter**

---

**G E O L O G I C A L   S U R V E Y   C I R C U L A R   6 7 2**

**United States Department of the Interior**

THOMAS S. KLEPPE, *Secretary*



**Geological Survey**

V. E. McKelvey, *Director*

First printing 1972

Second printing 1976

## CONTENTS

	Page
Abstract .....	1
Introduction .....	1
Seismic potential .....	2
Design approach .....	2
Ground motion values .....	3
Acceleration .....	4
Velocity .....	9
Displacement .....	10
Duration .....	11
References .....	13
Appendix A, Recurrence intervals .....	14
Appendix B, Procedure of Newmark and Hall for determination of response spectra .....	15
Appendix C, Ground motion data.....	15

## ILLUSTRATIONS

	Page
Figure 1. Map of proposed route of trans-Alaska oil pipeline showing seismic zonation and magnitudes of design earthquakes.....	2
2. Accelerogram from 1966 Parkfield earthquake illustrating definition of ground motion parameters.....	4
3 - 6 Graphs showing:	
3. Peak horizontal acceleration versus distance to slipped fault as a function of magnitude.....	5
4. Peak horizontal acceleration versus distance to slipped fault (or epicentral distance) for magnitude 5 earthquakes.....	6
5. Peak horizontal accelerations and 0.05g horizontal durations versus distance to slipped fault for 1966 Parkfield earthquake	7
6. Peak horizontal acceleration versus distance to slipped fault (or epicentral distance) for magnitude 6 earthquakes.....	8
7. Unfiltered and filtered accelerograms of the 1971 San Fernando earthquake .....	9
8 - 11 Graphs showing:	
8. Peak horizontal velocity versus distance to slipped fault (or epicentral distance) for magnitudes 5, 6, and 7.....	10
9. Peak horizontal dynamic displacement versus distance to slipped fault (or epicentral distance) for magnitudes 5, 6, and 7 .....	12
10. Duration of shaking versus distance to slipped fault (or epicentral distance) for magnitudes 5, 6, and 7.....	13
11. Examples of tripartite logarithmic ground and response spectra .....	15

## TABLES

	Page
Table 1. Design earthquakes along the pipeline route.....	2
2. Near-fault horizontal ground motion.....	3
3. Peak horizontal ground accelerations from filtered and unfiltered accelerograms at Pacoima dam.....	8
4. Peak ground acceleration data for which distances to the causative fault are most accurately known.....	16
5. Strong motion data plotted on graphs showing peak horizontal acceleration, velocity, and dynamic displacement and dura- tion of shaking as a function of distance to slipped fault (or epicentral distance).....	19



# Ground Motion Values for Use in the Seismic Design of the Trans-Alaska Pipeline System

---

By Robert A. Page, David M. Boore, William B. Joyner, and Henry W. Coulter

---

## ABSTRACT

The proposed trans-Alaska oil pipeline, which would traverse the state north to south from Prudhoe Bay on the Arctic coast to Valdez on Prince William Sound, will be subject to serious earthquake hazards over much of its length. To be acceptable from an environmental standpoint, the pipeline system is to be designed to minimize the potential of oil leakage resulting from seismic shaking, faulting, and seismically induced ground deformation.

The design of the pipeline system must accommodate the effects of earthquakes with magnitudes ranging from 5.5 to 8.5 as specified in the "Stipulations for Proposed Trans-Alaskan Pipeline System." This report characterizes ground motions for the specified earthquakes in terms of peak levels of ground acceleration, velocity, and displacement and of duration of shaking.

Published strong motion data from the Western United States are critically reviewed to determine the intensity and duration of shaking within several kilometers of the slipped fault. For magnitudes 5 and 6, for which sufficient near-fault records are available, the adopted ground motion values are based on data. For larger earthquakes the values are based on extrapolations from the data for smaller shocks, guided by simplified theoretical models of the faulting process.

## INTRODUCTION

The route of the proposed trans-Alaska oil pipeline from Prudhoe Bay on the Arctic Ocean to Valdez on Prince William Sound intersects several seismically active zones. Sections of the proposed pipeline will be subject to serious earthquake hazards, including seismic shaking, faulting, and seismically induced ground deformation such as slope failure, differential com-

paction, and liquefaction. This report is concerned only with seismic shaking that, if not accommodated in the design, could cause deformation leading to failure in the pipeline, storage tanks, and appurtenant structures and equipment and ultimately to the leakage of oil. It might also induce effects such as seicheing of liquids in storage tanks and liquefaction, landsliding, and differential compaction in foundation materials, all of which could result in deformation and potential failure.

To protect the environment, the pipeline system is to be designed so as to minimize the potential of oil leakage resulting from effects of earthquakes. The magnitudes of the earthquakes which the design must accommodate are given in "Stipulations for Proposed Trans-Alaskan Pipeline System" ([U.S.] Federal Task Force on Alaskan Oil Development, 1972, Appendix, Sec. 3.4.1, p. 55), hereinafter referred to as "Stipulations." This report characterizes ground motions for the specified design earthquakes.

The seismic design of the proposed pipeline involves a combination of problems not usually encountered. In the design of important structures, detailed geologic and soil investigations of the site generally provide the background data. Such detailed site investigations are not economically feasible for a linear structure nearly 800 miles long. In addition, a structure more limited in extent can be located on competent foundation materials and away from known

faults, whereas a pipeline traversing Alaska from north to south unavoidably crosses active faults and encounters a full range of foundation conditions from bedrock to water-saturated silty sands with a high potential for liquefaction (U.S. Geol. Survey, 1971).

### SEISMIC POTENTIAL

The "Stipulations" specify the earthquake potential along the proposed pipeline route in terms of design earthquakes in five broad seismic zones as given in table 1 and shown in figure 1. The zonation is based on the limited existing

mental records of shocks equal to the design earthquakes; elsewhere the design earthquakes exceed the largest recorded shocks. Recurrence intervals for the design earthquakes in the five zones from Valdez to Prudhoe Bay are estimated to be 200, 200, 200, 50 and 50 years (Appendix A).

Potential for surface or near-surface faulting must be assumed for the design earthquakes. Surface rupturing was associated with the great 1899 and 1964 shocks in the southern coastal seismic belt. Moreover, the available seismic data indicate that earthquakes along the pipeline route are shallow. The most reliable information is from detailed seismic studies near Fairbanks (Gedney and Berg, 1969) and at the Denali fault crossing (Page, 1971). Focal depths in these areas are less than 21 and 13 km (kilometers), respectively. There is no reliable evidence that earthquakes are substantially deeper elsewhere beneath the pipeline route.

In the absence of detailed geologic information to delineate active faults and to assess the seismic risk associated with each fault, the design of the pipeline must allow for the occurrence of the design earthquake anywhere within the seismic zone. In particular, the design must consider potential ground motion and deformation associated with earthquakes occurring at shallow depth in the immediate vicinity of the pipeline.

### DESIGN APPROACH

There are two common approaches to seismic design of a structure: One utilizes a complete time history of ground motion to evaluate dynamic behavior. The other, adopted for the design of the pipeline system (Alyeska Pipeline Service Co., 1971), is a quasi-static method in which seismically induced stresses are determined from structural response spectra for specified levels of ground motion.

Structural response spectra for the pipeline system are calculated in a three-step process. First, ground-motion values appropriate to the design earthquakes are specified. Then, design values of motion are derived by modifying the ground-motion values to implicitly allow for nonlinear, energy-absorbing mechanisms in the vibratory response of the structure, a step required by the assumption of purely elastic response, although the actual response is usually

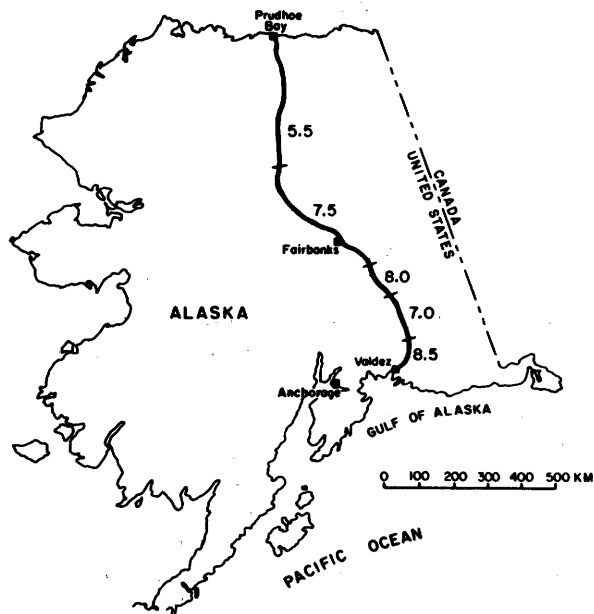


Figure 1.—Map of proposed route of trans-Alaska oil pipeline showing seismic zonation and magnitudes of design earthquakes.

seismic and geologic data and a rudimentary understanding of tectonic processes acting along the proposed route. If geologic and geophysical information along the route were sufficiently detailed, the zonation might be more refined and possibly less conservative.

Table 1.—Design earthquakes along the pipeline route

Seismic zone	Magnitude
Valdez to Willow Lake	8.5
Willow Lake to Paxson	7.0
Paxson to Donnelly Dome	8.0
Donnelly Dome to 67°N	7.5
67°N to Prudhoe Bay	5.5

The design earthquakes are maximum credible events in the sense that they are the largest shocks that are reasonably likely to occur over an interval of a few hundred years. Only for the magnitude 8.5 and 7.5 zones are there instru-

inelastic and nonlinear for large ground motions. Finally, smoothed tripartite logarithmic response spectra are constructed from the design seismic motions by the general procedure of Newmark and Hall (1969), outlined in Appendix B.

The initial step in the design process discussed herein characterizes ground motion appropriate to the design earthquakes. This step is based solely on seismological data and principles and does not incorporate factors dependent on soil-structure interactions, deformational processes within structures, or the importance of the structures to be designed. It involves scientific data and interpretation, whereas the subsequent steps involve engineering, economic, and social judgments relating to the nature and value of the structures.

The choice of parameters with which to specify ground motion was guided by the design approach adopted for the pipeline project. A useful set for the derivation of tripartite structural response spectra includes acceleration, velocity, displacement, and duration of shaking.

#### GROUND MOTION VALUES

Table 2 characterizes near-fault horizontal ground motion for the design earthquakes. The intensity of shaking is described by maximum values of ground acceleration, velocity, and displacement. In addition to the maximum acceleration, levels of absolute acceleration exceeded or attained two, five, and ten times are specified, because a single peak of intense motion may contribute less to the cumulative damage potential than several cycles of less intense shaking. Levels of absolute velocity exceeded or attained two and three times are also given.

There is substantial evidence that the duration of shaking strongly affects the extent of damage caused by an earthquake; yet the problem of how duration is related to magnitude has received little attention in the literature. In this study, the measure of duration used corresponds to the time interval between the first and last peaks of absolute acceleration equal to or larger than 0.05 g. Operational definitions of the acceleration and duration parameters are illustrated on an accelerogram in figure 2.

The values in table 2 are based on instrumental data insofar as possible. Strong-motion data have been obtained within 10 km of the causative fault for shocks as large as magnitude 6, but no accelerograms are available from within 40 km of the fault for a magnitude 7 shock and from within more than 100 km for a magnitude 8 shock. Estimates of intensity of near-fault ground motion for shocks larger than magnitude 6 are extrapolated from data obtained at larger distances or from near-fault data from smaller shocks.

The ground motion values in table 2 are subject to several conditions as follows. They are for a single horizontal component of motion. The intensity of shaking in the vertical direction is typically less than two-thirds that in a horizontal direction. They correspond to normal or average geologic site conditions and are not intended to apply where ground motion is strongly influenced by extreme contrasts in the elastic properties within the local geologic section. They characterize free-field ground motion, that is, ground motion not affected by the presence of structures. They contain no factor relating to the nature or importance of the structure

Table 2.—Near-fault horizontal ground motion

Magnitude	Acceleration (g) Peak absolute values				Velocity (cm/sec) Peak absolute values			Displacement (cm)	Duration <sup>1</sup> (sec)
	1st	2d	5th	10th	1st	2d	3d		
	8.5	1.25	1.15	1.00	0.75	150	130		
8.0	1.20	1.10	0.95	0.70	145	125	105	85	60
7.5	1.15	1.00	0.85	0.65	135	115	100	70	40
7.0	1.05	0.90	0.75	0.55	120	100	85	55	25
6.5	0.90	0.75	0.60	0.45	100	80	70	40	17
5.5	0.45	0.30	0.20	0.15	50	40	30	15	10

<sup>1</sup>Time interval between first and last peaks of absolute acceleration equal to or greater than 0.05 g.

Notes—1. Italic values are based on instrumental data.

2. The values in this table are for a single horizontal component of motion at a distance of a few (3-5) km of the causative fault; are for sites at which ground motion is not strongly altered by extreme contrasts in the elastic properties within the local geologic section or by the presence of structures; and contain no factor relating to the nature or importance of the structure being designed.
3. The values of acceleration may be exceeded if there is appreciable high-frequency (higher than 8 Hz) energy.
4. The values of displacement are for dynamic ground displacements from which spectral components with periods greater than 10 to 15 seconds are removed.

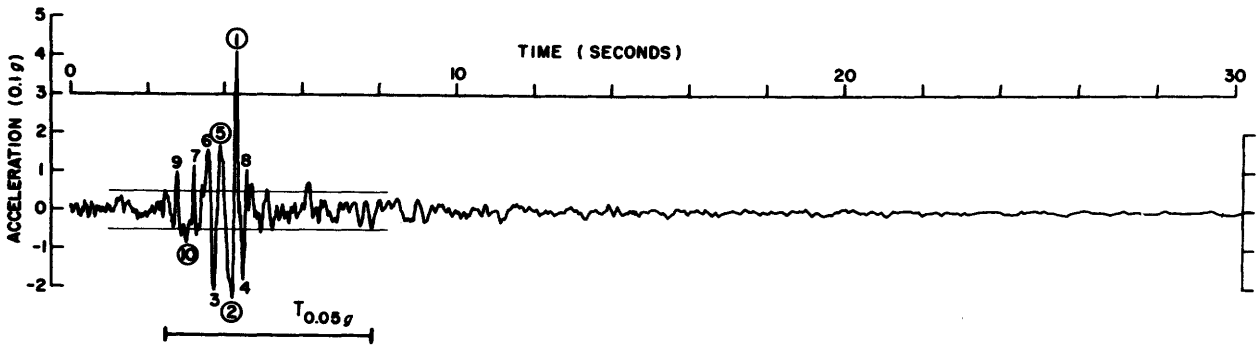


Figure 2.—Accelerogram from 1966 Parkfield earthquake illustrating definition of parameters referred to in table 2. Peaks on accelerogram are numbered consecutively 1 through 10 in order of decreasing amplitude. First, second, fifth, and tenth highest peaks are listed in table 2. Duration,  $T_{0.05g}$ , is the time interval between the first and last peaks of acceleration equal to or greater than 0.05 g in absolute value.

being designed. They are not the maximum possible. As mentioned in the following section, very little reliable data have been obtained within 10 km of the causative fault. How often these values are likely to be exceeded cannot be reliably estimated from the currently existing data. The acceleration values may be exceeded if there is appreciable energy in frequencies higher than 8 Hz (cycles per second). The displacement values correspond to dynamic ground displacements, as would be recorded on a strong-motion instrument having a frequency response flat to ground displacement for periods less than 10 to 15 seconds.

#### ACCELERATION

A plot of peak acceleration against shortest distance to the causative fault, including only those data for which source distances are most accurately known, reveals that peak acceleration increases with magnitude at all distances for which data exist and attenuates with distance  $r$  at a rate in the range  $r^{-1.5}$  to  $r^{-2.0}$  at distances beyond about 10 km for magnitude 5, about 20 km for magnitude 6, and less than 40 km for magnitude 7 (fig. 3).

For distances less than 10 km, there are no strong motion data for shocks larger than magnitude 6 and few reliable data for shocks of magnitude 5 and 6. The annual issues of "United States Earthquakes," published by the U.S. Coast and Geodetic Survey, list at least twelve magnitude 5 shocks and three magnitude 6 shocks in which strong motion records were obtained at epicentral distances of 16 km or less. For nearly all these events, the epicentral dis-

tance is uncertain by at least 5 to 10 km and for some possibly by as much as 25 km, and the actual slip surface is not known. Because of the rapid rate of attenuation, distance to the causative fault must be known to 1 or 2 km if the data are to be used to establish accelerations within a few kilometers of the fault.

Acceleration-distance data for magnitude 5 earthquakes recorded on one or more accelerographs within 32 km of the fault are plotted in figure 4. The most reliable and extensive near-fault data are from the 1966 Parkfield earthquake ( $m = 5.5$ ). Distances to the fault are unusually well determined for this event, the uncertainty being less than 0.5 km. The Parkfield data indicate a zone of little attenuation within about 10 km of the fault. In comparison with the other data for magnitude 5 shocks, the Parkfield data do not suggest anomalously intense shaking for that particular earthquake. In fact, the Parkfield data systematically lie beneath the points from the 1970 Lytle Creek earthquake ( $m = 5.4$ ); the discrepancy in accelerations for these two events probably reflects differences in seismic source parameters such as fault length and effective stress. The near-fault acceleration values in Table 2 for magnitude 5.5 are based on the Parkfield data, in particular, on the data recorded at a distance of 5 km. The regular variation of acceleration and duration with distance (fig. 5) suggests that the Parkfield data are free from anomalous local amplification of ground motion.

No near-fault accelerograms for an earthquake larger than about magnitude 6.6 are

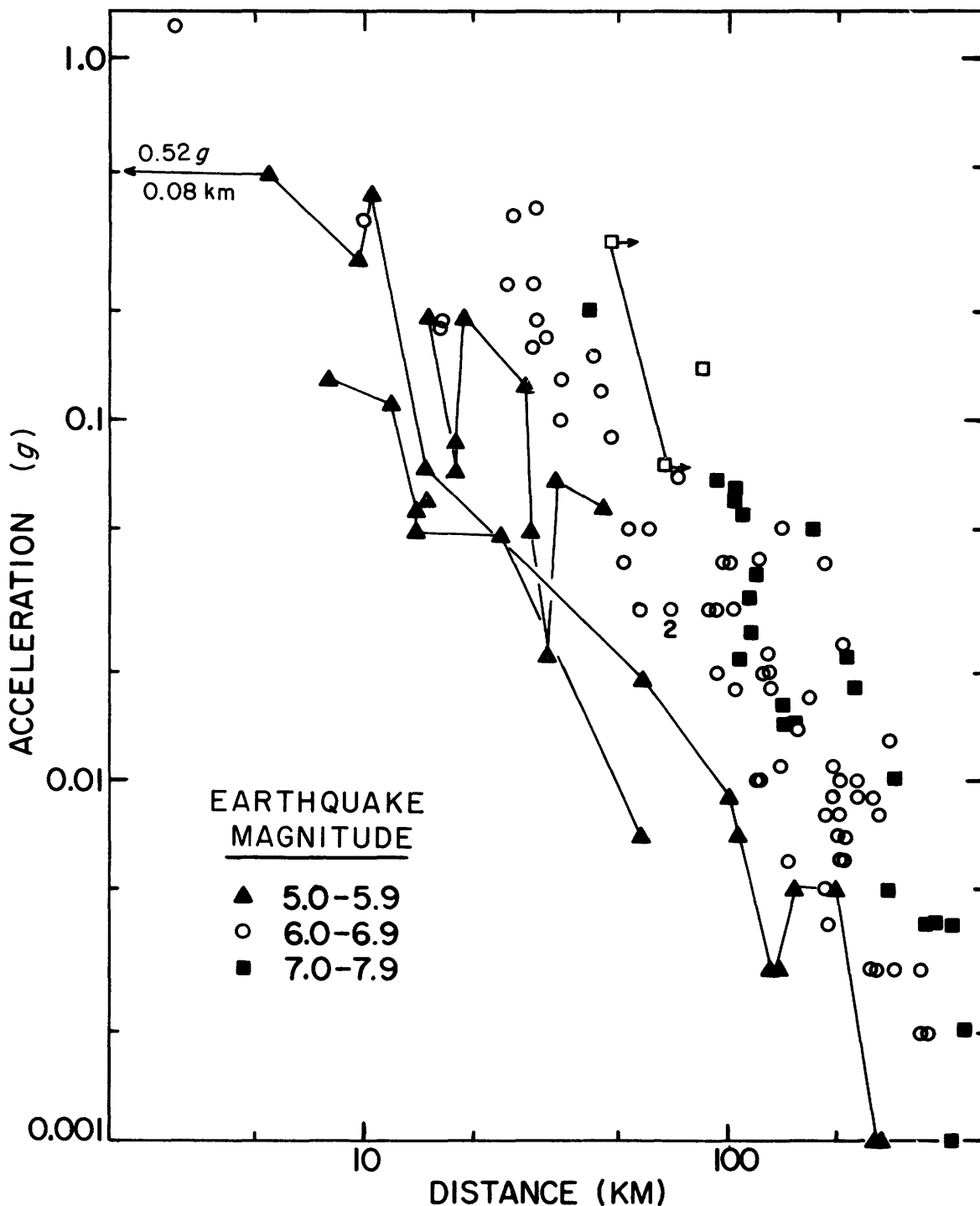


Figure 3.—Peak horizontal acceleration versus distance to slipped fault as a function of magnitude. Except for 1949 Puget Sound shock (open squares), data shown are those for which distances to fault are most accurately known (tabulated in Appendix C). Straight-line segments connect observations at different stations for an individual earthquake, for three magnitude 5 shocks and one magnitude 7 shock. From top to bottom, suites of magnitude 5 data are from 1970 Lytle Creek ( $m = 5.4$ ), Parkfield ( $m = 5.5$ ), and 1957 Daly City ( $m = 5.3$ ) shocks. Closest Parkfield data point lies off plot to left at 0.08 km. For magnitude 6, most data within 100 km are from 1971 San Fernando earthquake ( $m = 6.6$ ), and most data beyond 100 km are from 1968 Borrego Mountain earthquake ( $m = 6.5$ ). Most magnitude 7 data are from 1952 Kern County shock ( $m = 7.7$ ). Open squares are values from 1949 Puget Sound event ( $m = 7.1$ ), for which distances are determined to hypocenter assuming minimum focal depth of 45 km. Arrows denote minimum values.

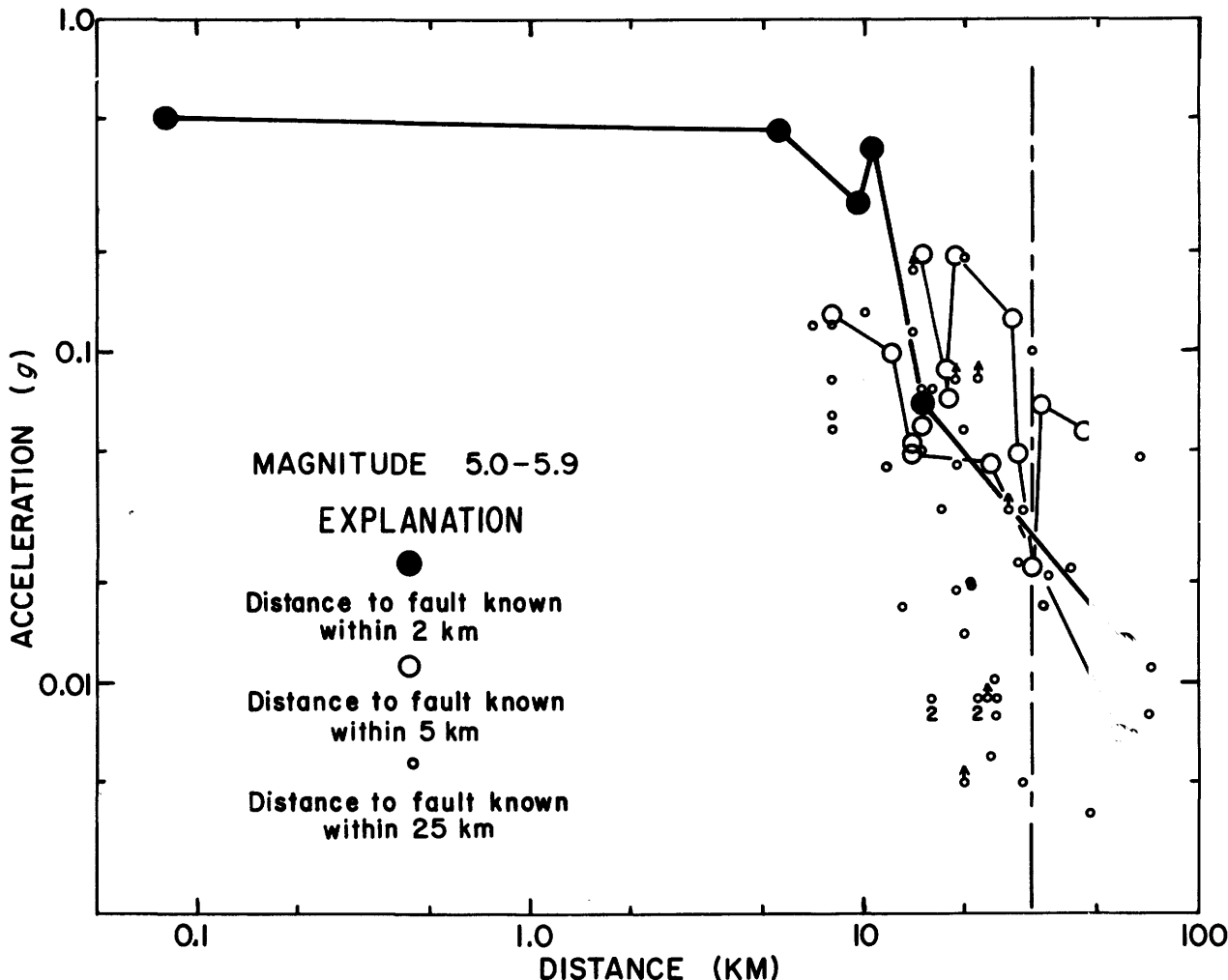


Figure 4.—Peak horizontal acceleration versus distance to slipped fault, if known, or epicentral distance for magnitude 5 earthquakes (Appendix C). Included are data from shocks in which at least one accelerogram was obtained within 32 km (dashed vertical line) of the fault or epicenter. No data beyond 100 km are plotted. Different symbols denote accuracy to which distance is known. Solid circles are 1966 Parkfield data for which distances to slipped fault are known to within 0.5 km. Large open circles are 1957 Daly City, 1967 Fairbanks, and 1970 Lytle Creek data for which distances to slipped surface are known to within 2-5 km. Small circles correspond to greater uncertainties in distance to source, possibly as large as 10-25 km. Line segments connect all data for individual events with better determined distances. Arrows denote minimum values.

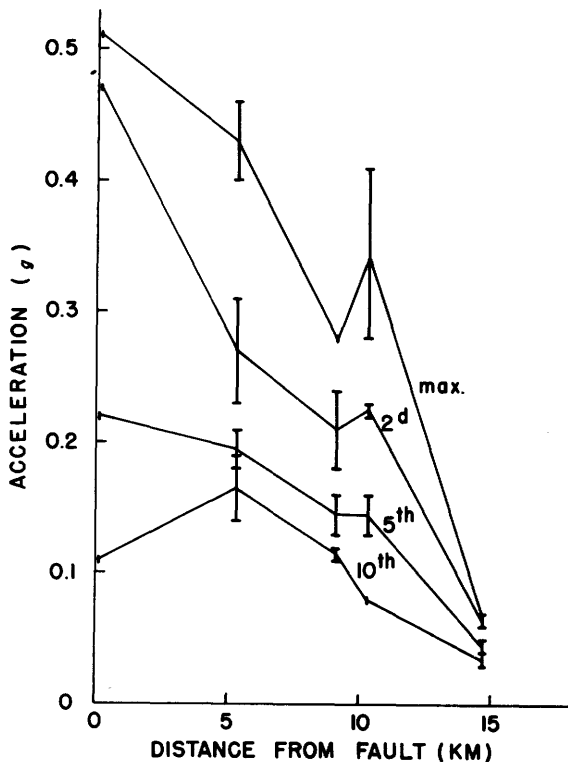
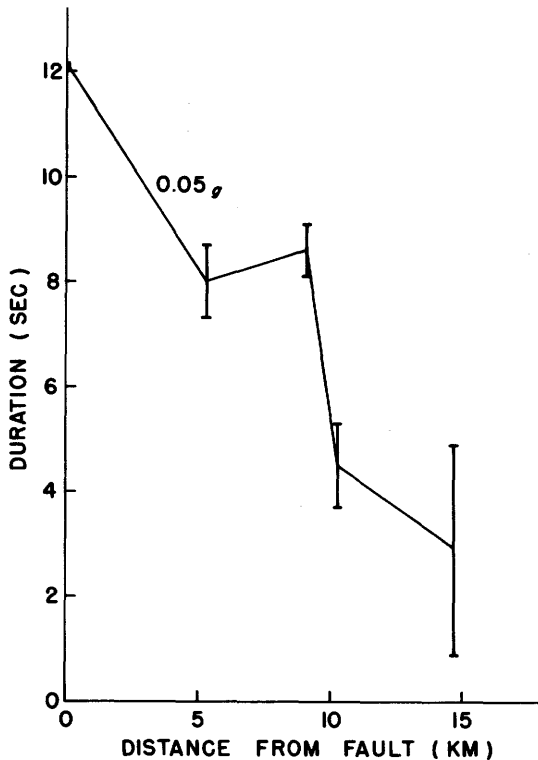
known to the authors. An accelerogram was obtained at a distance of about 10 km from the surface fault break in the 1940 Imperial Valley earthquake, which was given a surface-wave magnitude of 7.1 (Richter, 1958, p. 489); however, the character of the record indicates that this earthquake was a multiple event composed of a series of smaller shocks, the largest of which had a local Richter magnitude of about 6.4 (Trifunac and Brune, 1970). Accordingly, the recorded accelerations are more representative of a magnitude 6.5 shock, whereas the dura-

tions are more characteristic of a 7.0 event.

Acceleration-distance data for magnitude 6 earthquakes are plotted in figure 6. The only data for which the distance to the fault is known to an accuracy of 1 to 2 km are from the 1971

Figure 5.—Peak horizontal accelerations and 0.05g horizontal durations versus distance from slipped fault for 1966 Parkfield earthquake. Values of the first, second, fifth, and tenth highest absolute peaks of acceleration are shown. Where two horizontal components are available, both values are indicated by top and bottom of vertical bars. Only those data from within 15 km of the fault are shown.

San Fernando earthquake ( $m = 6.6$ ). This shock produced one accelerogram at a distance of about 3 km from the inferred slip surface and



more than 100 accelerograms at distances beyond 15 km. The peak acceleration from Pacoima at 3 km lies beneath a straight-line extrapolation of the trend of the data beyond 10 km; this behavior is consistent with a zone of little attenuation near the fault as observed for the Parkfield data in figure 4.

The maximum acceleration from the San Fernando earthquake was 1.25 g, nearly double the maximum acceleration recorded during any earthquake prior to 1971. The acceleration was recorded at a bedrock site adjacent to the Pacoima dam. Because the Pacoima accelerations are so much higher than those recorded in previous earthquakes, the question has arisen whether or not the record might be anomalous in the sense that the motion may have been significantly amplified by various site factors such as the rugged topographic relief, the presence of the dam, and the cracking and minor landsliding near the station. The authors are not aware of any investigations of possible site effects that conclusively demonstrate an anomalous amplification (greater than 25-50 percent) of recorded motion in the frequency range 1-10 Hz. The Pacoima ground motion in the period range 1 to 2 seconds is not inconsistent with that predicated from a simple theoretical fault model for the earthquake (Trifunac, 1972).

The near-fault acceleration values for magnitude 6.5, table 2, were derived from the Pacoima accelerograms of the San Fernando earthquake. In the Newmark and Hall method for estimating velocity response spectra (Appendix B), the spectral amplitude in the approximate frequency range 2-8 Hz is directly proportional to the peak ground acceleration. If the peak acceleration is dominated by higher frequency energy, the Newmark and Hall method overestimates the spectrum in this range. Frequencies higher than 8 Hz contributed significantly to the peak accelerations recorded at Pacoima (fig. 7); accordingly, the accelerograms were filtered to remove frequencies higher than about 9 Hz. Filtering reduced the accelerations by about 25 percent, as seen in table 3 and fig. 7. The near-fault acceleration values of table 2 for magnitude 6.5 were adopted from the filtered values.

Near-fault accelerations for magnitudes larger than 6.5 were extrapolated from strong mo-

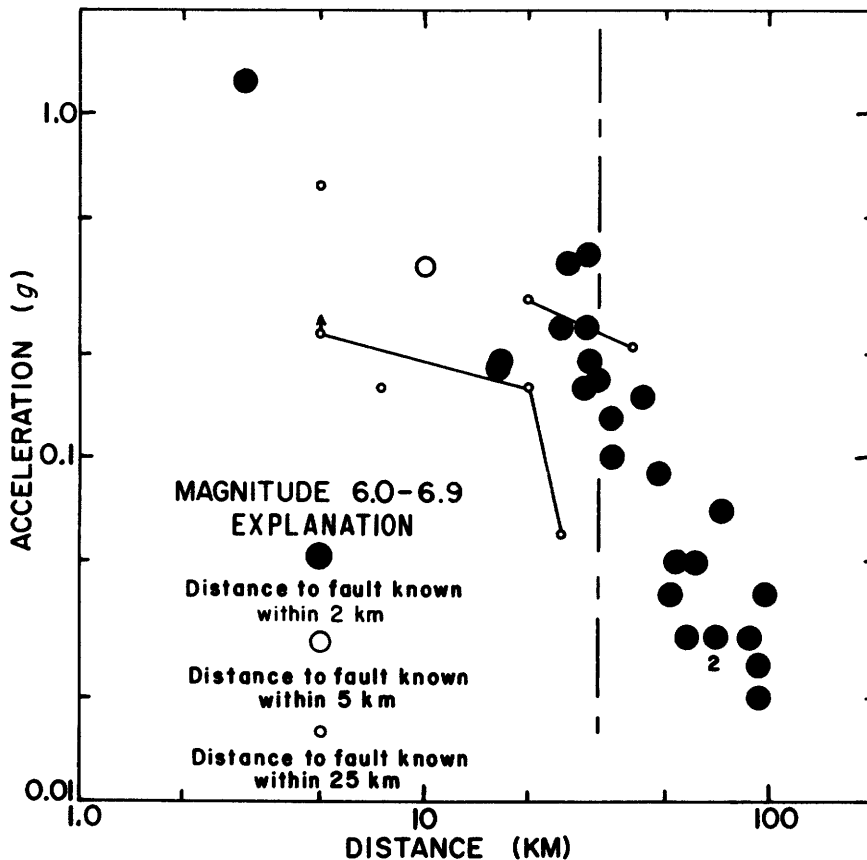


Figure 6.—Peak horizontal acceleration versus distance to slipped fault, if known, or epicentral distance for magnitude 6 earthquakes (Appendix C). Included are data from shocks in which at least one accelerogram was obtained within 32 km (dashed vertical line) of the fault or epicenter. Different symbols denote accuracy to which distance is known. Line segments connect data for individual shocks except for San Fernando data. Arrows denote minimum values.

tion observations at distances greater than 40 km and from the near-fault data from smaller shocks. The extrapolation was guided by two considerations. First, the existing strong motion data indicate that peak acceleration increases with magnitude at all distances for which data exists (fig. 3). Second, theoretical arguments (Brune, 1970) suggest that near-fault peak acceleration is proportional to the effective stress available to cause slippage and to the high-frequency cutoff in the recorded signal. Allowing for an increase of effective stress with magni-

tude, a value of 1.25 g was adopted for magnitude 8.5, and the values for intermediate magnitudes were interpolated between 1.25 g and the value of 0.9 g for magnitude 6.5. The numerous reports of shattered ground and of rocks and objects apparently thrown into the air in the epicentral region of large earthquakes (for example, Richter, 1958, p. 25-26, 50-51; Morrill, 1971; Barrows and others, 1971) are consistent with accelerations of 1 g and greater, although various alternative mechanisms that might produce such effects from less intense shaking have been offered in many instances (Richter, 1958, p. 25-26). The acceleration values adopted in Table 2 increase markedly between magnitude 5.5 and 6.5 and then less rapidly with magnitude above 6.5.

TABLE 3.—Peak horizontal ground accelerations from filtered and unfiltered accelerograms at Pacoima dam

Component		1st	2nd	5th	10th
S 74° W.	unfiltered	1.25 g	1.15 g	0.69 g	0.57 g
	filtered	.82	.77	.59	.44
S 16° E.	unfiltered	1.22	1.01	.79	.52
	filtered	.93	.77	.60	.45

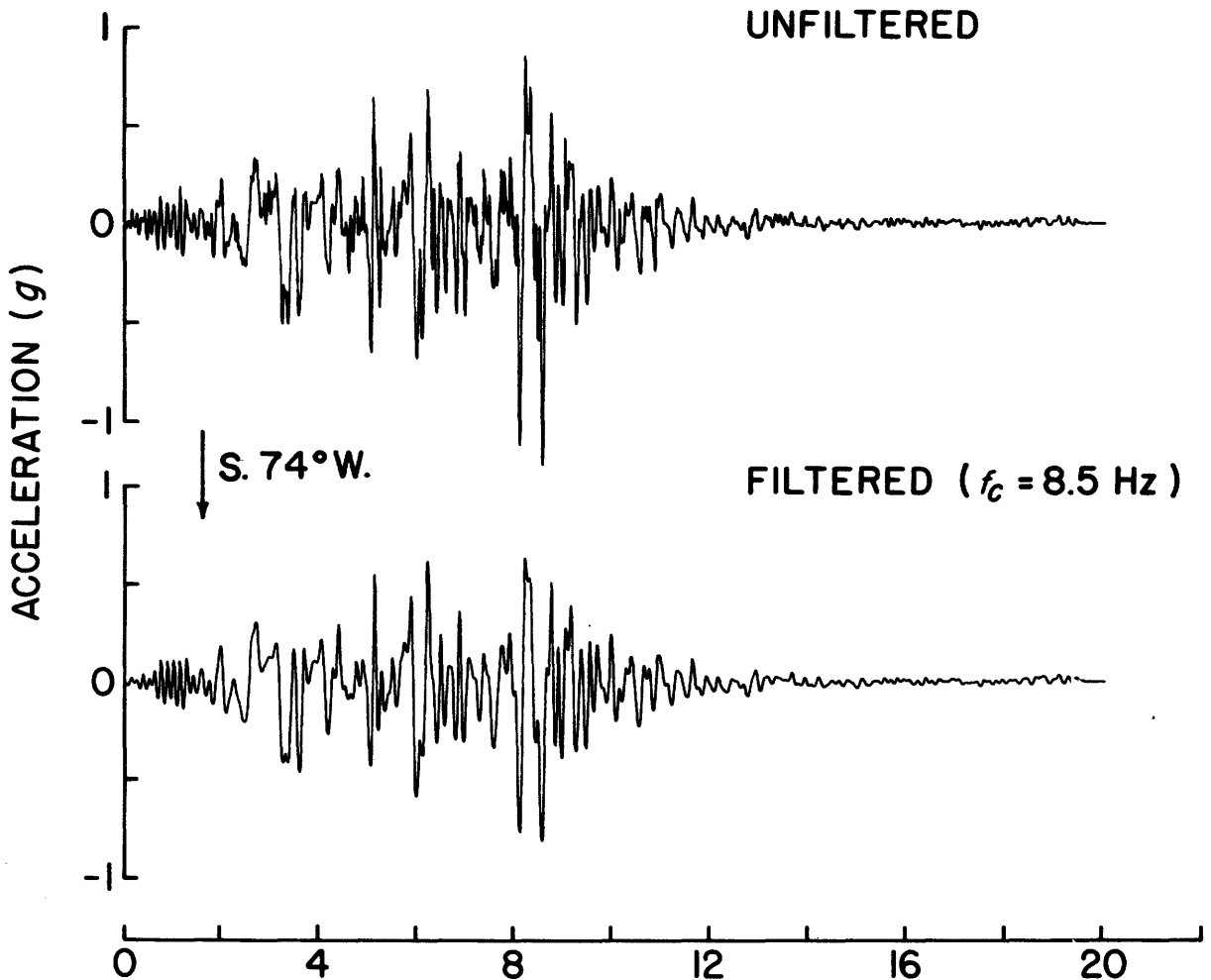


Figure 7.—Unfiltered and filtered accelerograms of the 1971 San Fernando earthquake from the S. 74° W. accelerograph component at Pacoima dam. Response of filter is 1.0 at frequencies less than 8 Hz and 0.0 at frequencies greater than 9 Hz with a half-wave cosine taper from 8 to 9 Hz.

#### VELOCITY

The response curve of the standard strong motion seismograph operated in the United States is flat to acceleration over the frequency range of the predominant ground motion. Accordingly, accelerations are measured directly from the strong motion recordings, whereas velocities are obtained by integration of the record. For this reason, there are few velocity data in the literature relative to acceleration data.

Peak velocity data in the magnitude range 5-7 plotted as a function of distance from the source (fig. 8) indicate that peak velocity increases with magnitude at all distance for which data exist. Those data points for which distance

to the fault is accurately known (large symbols) tend to separate according to magnitude; the remaining data confirm this tendency, although their behavior is somewhat obscured by scatter arising at least partially from errors in distances. The plot reveals that beyond about 10 km, peak velocity attenuates less rapidly with distance than peak acceleration.

The near-fault velocity values for magnitude 5.5 (table 2) are averages of the Parkfield values recorded at 0.08 and 5.5 km from the fault. The values for magnitude 6.5 are based on the San Fernando observations at the Pacoima site about 3 km from the fault surface. For the larger magnitudes, the values were extrapolated from those for 5.5 and 6.5 on the as-

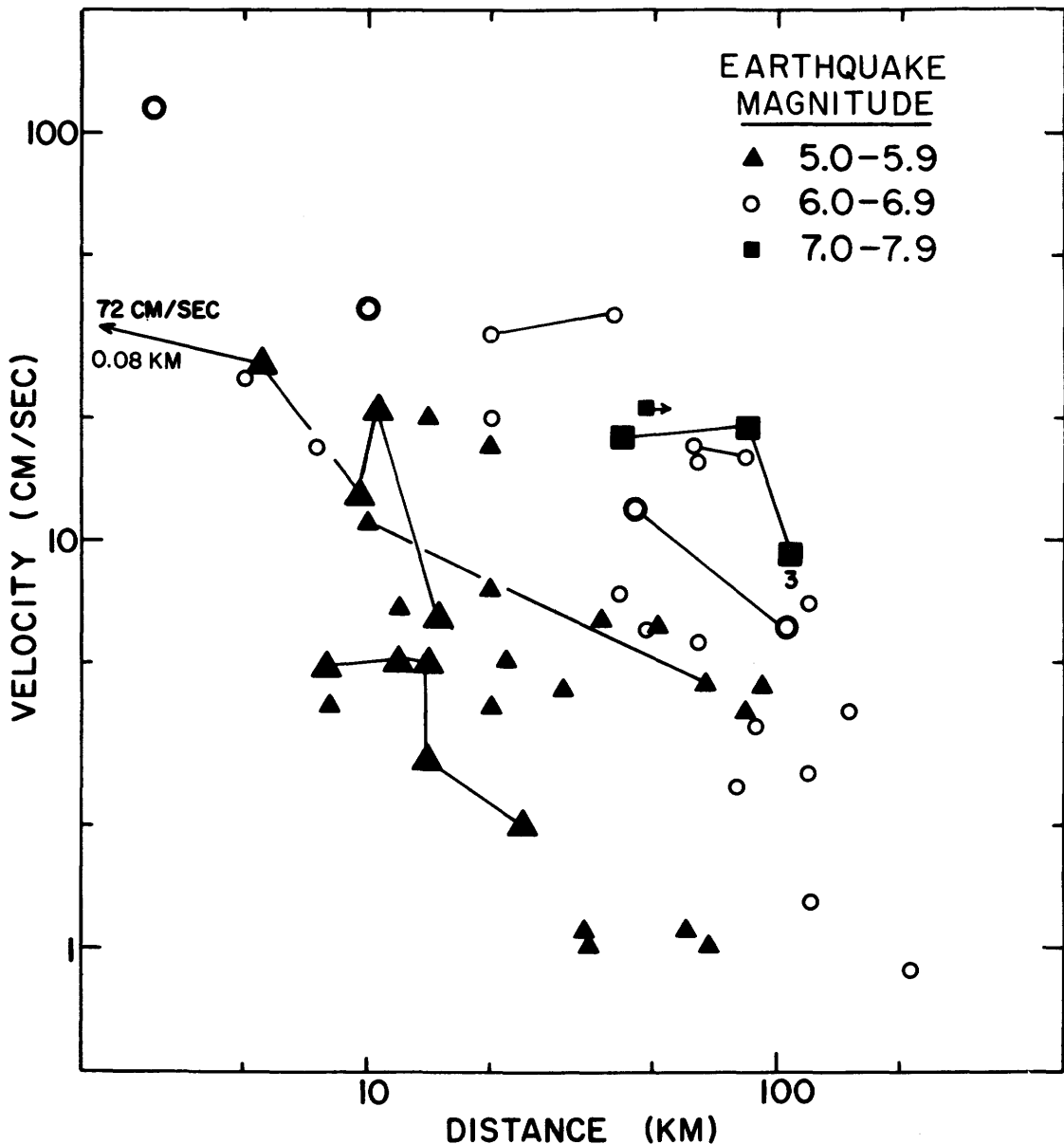


Figure 8.—Peak horizontal velocity versus distance to slipped fault, if known, or epicentral distance for magnitudes 5, 6, and 7 (tabulated in Appendix C). Uncertainties in distances are less than 5 km for larger symbols and more than 5 and possibly as large as 25 km for smaller symbols. Line segments connect data for individual shocks. The closest point to the fault for the Parkfield shock lies off the plot at 0.08 km. Arrows denote minimum values.

sumption that near-fault velocities increase with magnitude, corresponding to an increase in effective stress with magnitude. A peak value of 150 cm/sec (centimeters per second) was assumed for magnitude 8.5, and the intervening values were interpolated. Prior to the San Fernando earthquake, theoretical estimates of an upper limit for near-fault peak velocity were in the range 100-150 cm/sec (Ambraseys, 1969;

Brune, 1970). A velocity of 115 cm/sec was recorded at the Pacoima site during the San Fernando earthquake ( $m=6.6$ ); hence the assumed value of 150 cm/sec for magnitude 8.5 is considered reasonable.

#### DISPLACEMENT

Instrumental data on peak dynamic displacements are less reliable than the data for either peak accelerations or velocities. Data on dy-

dynamic displacements excluding spectral components with periods greater than about 10-15 seconds are available from double integration of accelerograms or directly from displacement meters. Both types of data are subject to uncertainties. In the double integration of digitized accelerograms, errors may arise from low-frequency noise in the digitization of the original accelerogram and from lack of knowledge of the true baseline of the accelerogram. On the other hand, there are instrumental difficulties associated with displacement meters operating with a free period of 10 seconds. The relative accuracy of the two types of data is not adequately understood (Hudson, 1970).

Peak displacement data obtained from double integration of accelerograms and from 10-second displacement meters when plotted against distance (fig. 9) show no apparent systematic difference between the two types of data within the scatter of the points. Peak displacement at a given distance from the fault, like peak acceleration and velocity, increases with magnitude.

The near-fault value of peak displacement for magnitude 5.5 (table 2) is the mean of the Parkfield values obtained at 0.08 and 5.5 km from the fault. For magnitude 6.5 the value is based on the Pacoima record for the San Fernando earthquake. How peak dynamic displacement (for periods less than 10-15 seconds) scales with magnitude for larger shocks is uncertain. An upper limit to the increase of near-fault dynamic displacement with magnitude is the rate at which fault dislocation increases with magnitude. The total fault slip in the 1964 Alaska shock ( $m=8.5$ ) is estimated to have been about five times that in the 1971 San Fernando earthquake ( $m=6.5$ ). Hence, an upper bound on the peak dynamic displacement for magnitude 8.5, after removal of low frequency energy, is about 2 m. In this study, a value of 1 m is assumed for magnitude 8.5, and the values between magnitude 6.5 and 8.5 are smoothly interpolated.

#### DURATION

The measure of duration used in this study is the time interval between the first and last acceleration peaks equal to or greater than 0.05 g. Although crude, this measure is readily applied to the existing accelerograms and approximates the cumulative time over which the ground accelerations exceed a given level. Comparison of felt reports for earthquakes of mag-

nitude 5 and 6 with near-fault accelerograms from shocks of similar magnitude suggest that the "intense" or "strong" phase of shaking mentioned in felt reports corresponds to accelerations of about 0.05 g and greater. In comparison, the minimum perceptible level of acceleration is 0.001 g (Richter, 1958, p. 26).

Durations obtained for several earthquakes in the magnitude range 5-7 indicate that for a given magnitude, duration decreases with increasing distance from the source, and that at a given distance from the source, duration increases for larger magnitudes (fig. 10). The 0.05 g duration for magnitude 5.5 (table 2) is the mean of the maximum durations for the 1966 Parkfield shock ( $m = 5.5$ ) recorded at distances of 0.08 and 5.5 km from the fault surface (fig. 5). The durations for magnitude 6.5 and 7.0 are based respectively on the measured 0.05 g durations of 13 seconds at Pacoima dam in the 1971 San Fernando earthquake ( $m = 6.6$ ) and of 30 seconds at El Centro in the 1940 Imperial Valley earthquake, which was a multiple event characterized by a surface-wave magnitude of 7.1. These data were smoothed slightly to obtain a regular increase of duration with magnitude in table 2. The adopted near-fault durations of 17 and 25 seconds for magnitudes 6.5 and 7.0 are consistent with the duration data in figure 10 within the scatter of the points.

In the absence of near-fault data for larger magnitudes, durations can be estimated from theoretical calculations in corroboration with felt observations. Assume that a magnitude 8.5 earthquake is a multiple event comprised of several shocks as large as magnitude 7.5 distributed along a fault 500-1,000 km in length. Peak accelerations of 0.05 g or greater are expected for a magnitude 7.5 earthquake at distances up to 100 km (fig. 3). For a rupture propagation velocity of 2 to 3.5 km/sec, the 0.05 g duration at a near-fault station near the center of the fault would be 100 to 57 seconds, respectively. In comparison, felt reports of the duration of intense shaking in the aftershock zone of the 1964 Alaska earthquake ( $m = 8.5$ ) ranged from 60-90 seconds at Whittier (Kachadoorian, 1966) to 150 seconds at Kodiak (Kachadoorian and Plafker, 1967). The tabulated duration of 90 seconds for magnitude 8.5 (table 2) is consistent with the calculated range of values and with felt data from the 1964 shock.

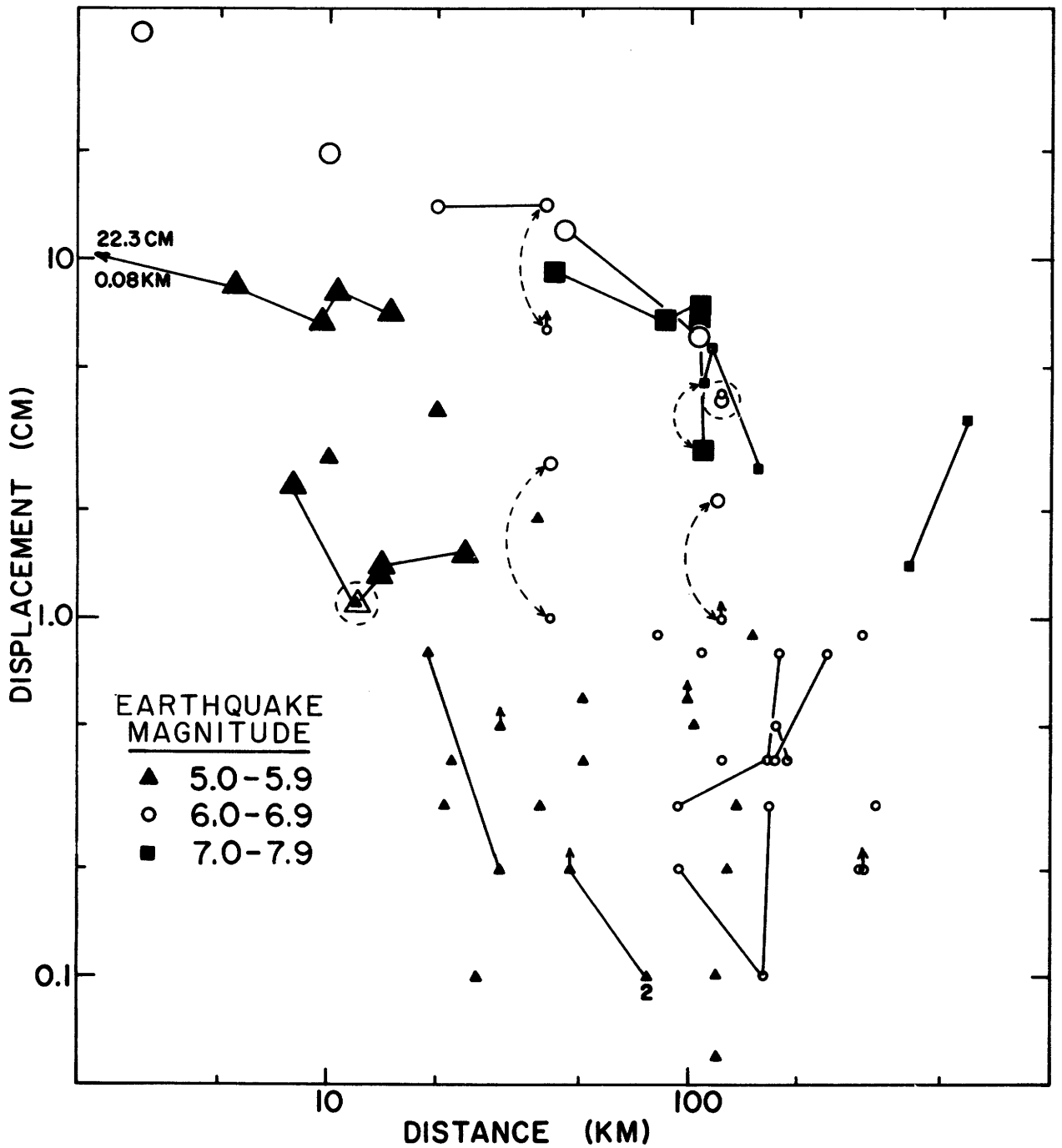


Figure 9.—Peak horizontal dynamic displacement for spectral components with periods less than 10-15 seconds versus distance to slipped fault, if known, or epicentral distance for magnitudes 5, 6, and 7 (tabulated in Appendix C). Small symbols are data from 10-second displacement meters. Larger symbols are data from double integration of accelerograms, with largest symbols for distances uncertain by less than 5 km and the intermediate symbols for uncertainties of 5 to possibly 25 km. Line segments join data from individual shocks. Dashed curves connect and dashed circles enclose values for same site and component obtained from the two different sources. Arrows denote minimum values.

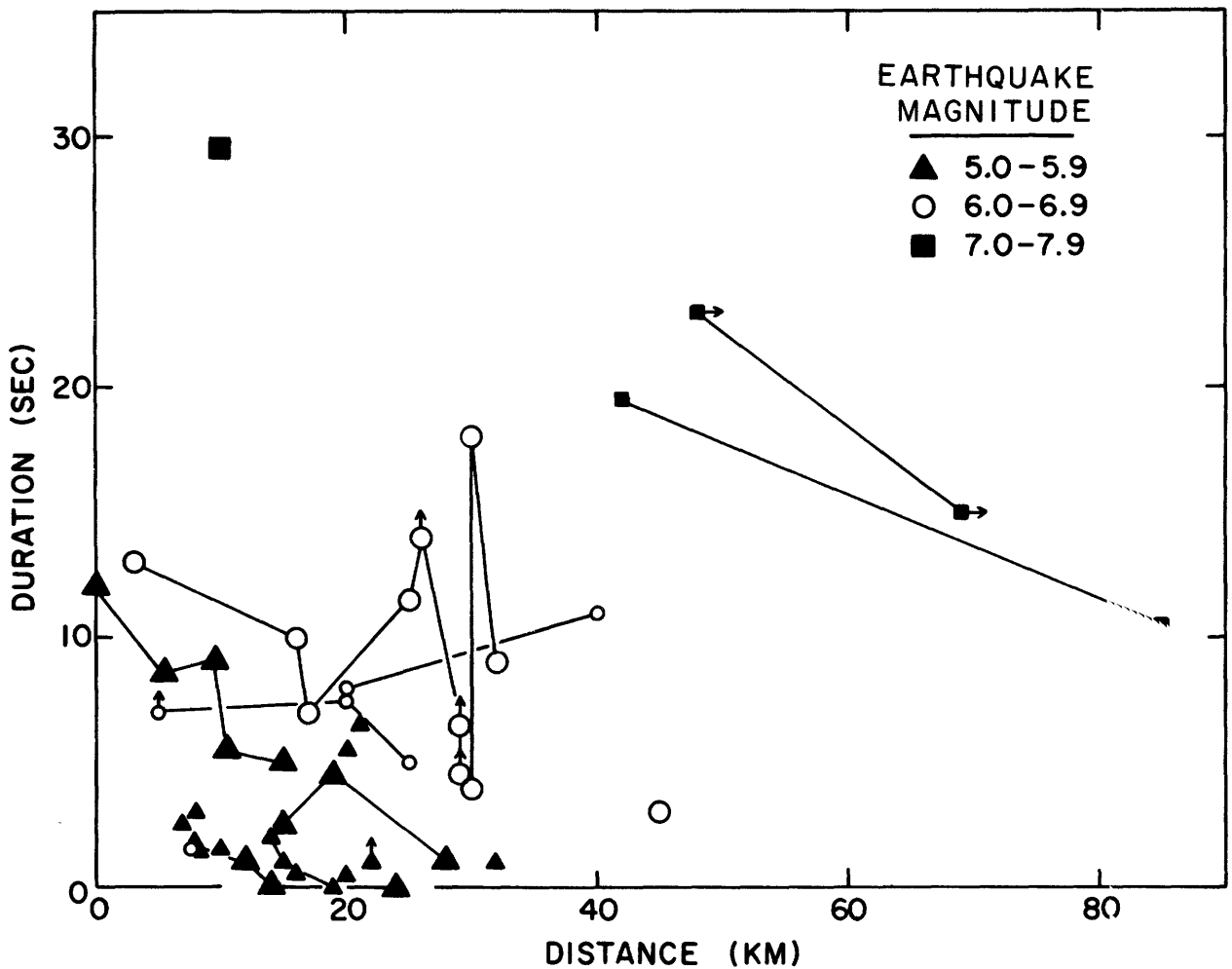


Figure 10.—Duration of shaking versus distance to slipped fault, if known, or epicentral distance for magnitudes 5, 6, and 7. Shown is 0.05g duration (see fig. 2 for definition; plotted data are tabulated in Appendix C). Distances represented by larger symbols are uncertain by less than 5 km; those indicated by smaller symbols by 5 to possibly 25 km. Arrows denote minimum values.

The durations for magnitude 7.5 and 8.0 were interpolated between the values for magnitudes 7.0 and 8.5 to obtain a smooth increase in duration with magnitude.

#### REFERENCES

- Alyeska Pipeline Service Company, 1971, Alignment sheet 65 design, Appendix A-3.1023 of Project description of the trans-Alaska pipeline system: Houston, Texas, Alyeska Pipeline Service Co., 92 p.
- Ambraseys, N. N., 1969, Maximum intensity of ground movements caused by faulting: Fourth World Conference on Earthquake Engineering, Santiago, Chile, 1967, Proc., v. 1, p. 154-171.
- Barrows, A. G., Kahle, J. E., Weber, F. H., and Saul, R. B., 1971, Map of surface breaks resulting from the San Fernando, California, earthquake of February 9, 1971: California Div. Mines and Geology Prelim. Rept. No. 11, plate 1.
- Brune, J. N., 1970, Tectonic stress and the spectra of seismic shear waves from earthquakes: Jour. Geophys. Research, v. 75, p. 4997-5009.
- Gedney, L., and Berg, E., 1969, The Fairbanks earthquakes of June 21, 1967: Aftershock distribution, focal mechanisms, and crustal parameters: Seismol. Soc. America Bull., v. 59, p. 73-100.
- Hastie, L. M., and Savage, J. C., 1970, A dislocation model for the 1964 Alaska earthquake: Seismol. Soc. American Bull., v. 60, p. 1389-1392.
- Hudson, D. E., 1970, Ground motion measurements: in Wiegell, R. L., (ed.) Earthquake Engineering: Englewood Cliffs, N.J., Prentice-Hall, p. 107-125.
- Hudson, D. E., Brady, A. G., Trifunac, M. G., and Vijayaraghavan, A., 1971, Strong-motion earthquake accelerograms, digitized and plotted data, Volume 2, A: California Inst. Technology, Earthquake Eng. Research Lab. Rept. 71-50, p. 321.
- Kachadoorian, R., 1966, Effects of the earthquake of March 27, 1964 at Whittier, Alaska: U.S. Geol. Survey Prof. Paper 542-B, 21 p.

- Kachadoorian, R., and Plafker, G., 1967, Effects of the earthquake of March 27, 1964 on the communities of Kodiak and nearby islands: U.S. Geol. Survey Prof. Paper 542-F, 41 p.
- Morrill, B. J., 1971, Evidence of record vertical accelerations at Kagel Canyon during the earthquake, in *The San Fernando, California, earthquake of February 9, 1971*: U.S. Geol. Survey Prof. Paper 733, p. 177-181.
- Newmark, N. M., and Hall, W. J., 1969, Seismic design criteria for nuclear reactor facilities: Fifth World Conference on Earthquake Engineering, Santiago, Chile, 1967, Proc., v. 2, p. 37-50.
- Page, R. A., 1971, Microearthquakes on the Denali fault near the Richardson Highway, Alaska [abs.]: *Am. Geophys. Union Trans.*, v. 52, p. 278.
- 1972, Crustal deformation on the Denali fault, Alaska, 1942-1970: *Jour. Geophys. Research*, v. 77, p. 1528-1533.
- Plafker, G., 1969, Tectonics of the March 27, 1964 Alaska earthquake: U.S. Geol. Survey Prof. Paper 543-I, p. 174.
- Richter, C. F., 1958, *Elementary Seismology*: San Francisco, W. H. Freeman and Co., 768 p.
- Richter, D. H. and Matson, N. A., 1971, Quaternary faulting in the eastern Alaska Range: *Geol. Soc. America Bull.*, v. 82, p. 1529-1539.
- Stout, J. H., Brady, J. B., Weber, F., and Page, R. A., 1972, Evidence for Quaternary movement on the McKinley strand of the Denali fault in the Delta River area, Alaska: *Geol. Soc. America Bull.* (in press).
- Sykes, L. R., 1972, Aftershock zones of great earthquakes, seismicity gaps, and earthquake prediction for Alaska and the Aleutians: *Jour. Geophys. Research*, v. 76, p. 8021-8041.
- Trifunac, M. D., 1972, Stress estimates for the San Fernando, California, earthquake of February 9, 1971: Main event and thirteen aftershocks: *Seismol. Soc. America Bull.*, v. 62, p. 721-750.
- Trifunac, M. D., and Brune, J. N., 1970, Complexity of energy release during the Imperial Valley, California earthquake of 1940: *Seismol. Soc. America Bull.*, v. 60, p. 137-160.
- [U.S.] Federal Task Force on Alaskan Oil Development, 1972, Introduction and summary, v. 1 of Final environmental impact statement, proposed trans-Alaska pipeline: U.S. Dept. Interior interagency rept., 386 p.; available only from the Natl. Tech. Inf. Service, U.S. Dept. Commerce, Springfield, Va., NTIS PB-206921-1.
- U.S. Geological Survey, 1971, Preliminary engineering geologic maps of the proposed trans-Alaska pipeline route [compiled by O. J. Ferrians, R. Kachadoorian, and F. R. Weber]: U.S. Geol. Survey open-file report.
- Wiggins, J. H., 1964, Effect of site conditions on earthquake intensity: *American Soc. Civ. Eng., Structural Div.*, v. 90, p. 279-313.

## APPENDIX A—RECURRENCE INTERVALS

Estimates of recurrence intervals for the design earthquakes are based on the historic seismic record and tectonic arguments. In the interpretation of the seismic history, the width of each seismic zone transverse to the pipeline route is assumed to be equal to the characteristic length of faulting for the specified magni-

tude.

In the southern coastal zone, earthquakes as large as the design earthquakes occurred in 1899 near Yakutat Bay and in 1964 in Prince William Sound. This pattern is consistent with a recurrence interval of less than 100 years; however, tectonic considerations indicate that the average long-term interval between design earthquakes is longer. In the framework of global tectonics, the 12 m of thrusting involved in the 1964 earthquake (Hastie and Savage, 1970) would require 200 years of strain accumulation at the local convergence rate of 6 cm/yr (centimeters per year) for the Pacific and North American plates. Geologic evidence of vertical movements in Prince William Sound (Plafker, 1969) indicates episodes of tectonic deformation between quiescent periods of the order of 800 years. On Middleton Island the total uplift in each deformational episode is 2.5-3 times that for the 1964 earthquake. The geologic evidence suggests a long-term average recurrence interval of about 300 years for an event comparable to the 1964 earthquake. An interval of 200 years is adopted for the magnitude 8.5 zone. The lack of seismic activity in the area between Yakutat Bay and the 1964 aftershock zone during the past 50 years has led Sykes (1972) to identify this part of the Aleutian-Alaskan seismic belt as a likely site of a future earthquake larger than magnitude 7.

The magnitude 8.0 zone includes the Denali fault system, an active strike-slip system that displays geologic evidence for an average Holocene slip rate of at least 3 cm/yr (Richter and Matson, 1971). Assumption of a 6-m offset for a magnitude 8.0 event and a 3 cm/yr slip rate gives a recurrence interval of 200 years. The lack of observable fault-slip and teleseismically recorded earthquakes on the fault system in the vicinity of the pipeline route and to the east indicates that the fault system has been effectively locked for at least 30 years (Page, 1972). An undeformed neoglacial moraine lying athwart the recently active fault trace is evidence that no major episode of faulting has occurred within the past 170 years (Stout and others, 1972).

Understanding of the tectonic framework of the magnitude 7.5 zone is not adequate for estimating recurrence intervals. One shock ap-

proaching the design magnitude has occurred on the pipeline route in this century, a magnitude 7.3 shock in 1937. A recurrence interval of 50 years is assumed.

In the magnitude 7.0 and 5.5 zones, there is no historic record of shocks as large as the design earthquakes. For the Willow Lake to Paxson zone, the record of earthquakes equal to or larger than magnitude 7.0 is probably complete for at least 50 years. From 67° N to Prudhoe Bay, the record for events as small as magnitude 5.5 is possibly complete since 1935, when a seismic station was established at College. Recurrence intervals of 200 and 50 years are assumed for the two zones.

#### APPENDIX B—PROCEDURE OF NEWMARK AND HALL FOR DETERMINATION OF RESPONSE SPECTRA

A response spectrum for a given level of damping is defined by the maximum responses (usually expressed in terms of displacement, velocity, or acceleration) of linear, single-degree-of-freedom oscillators (with different free periods but identical values of damping) when subjected to a specified time history of ground motion. A single spectrum is a plot of the maximum responses as a function of oscillator period or frequency; there is a different response spectrum for each level of damping. The usefulness of the response spectrum comes from the ability to model engineering structures by equivalent simple damped oscillators and to estimate stresses induced by the particular ground motion from knowledge of the equivalent period and damping of the structure and of the appropriate response spectrum.

The values of parameters describing the actual ground motion may be modified for non-linear energy-absorbing mechanisms before being used in the construction of a response spectrum. In the following example of the Newmark and Hall method for constructing response spectra, the ground motion values are not modified. The example is illustrative only of the general method and not of an application to a specific problem.

Response spectra calculated from accelerograms often contain many peaks and troughs, hence prudent design requires the use of an

envelope of the actual response spectrum. Newmark and Hall (1969) describe a graphical method for determining envelope response spectra. First a tripartite logarithmic "ground motion spectrum" is constructed with three lines representing ground displacement, velocity, and acceleration. These lines are then shifted upward on tripartite log paper, by amounts depending on damping, to reflect the dynamic amplification of the ground motion in the structure. The amounts by which the lines are shifted are derived empirically from recorded accelerograms and are subject to revision as new data become available. This procedure, using the amplification factors given by Newmark and Hall (1969), is illustrated in figure 11, where the velocity response spectrum for 2 per-

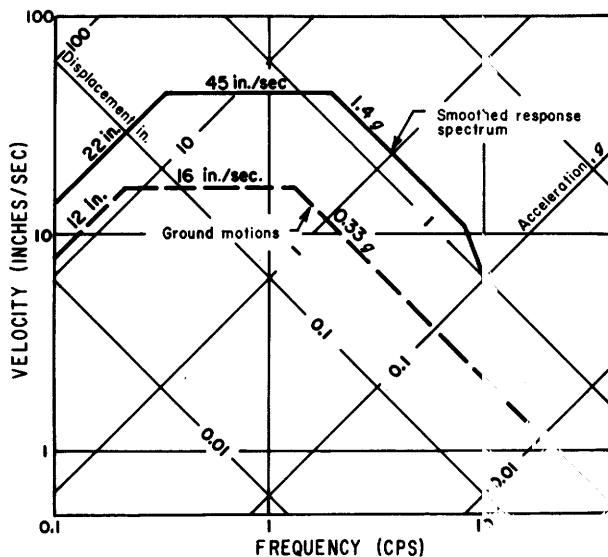


Figure 11.—Example of tripartite logarithmic ground (dashed) and response (solid) spectra (after Newmark and Hall, 1969). Accelerations and displacements may be read from the plot in addition to velocities. Response spectrum is for damping value of 2 percent of critical.

cent damping is estimated for a ground motion characterized by ground displacement of 12 inches, velocity of 16 inches per second, and acceleration of 0.33 g. At high and low frequencies, the response spectrum must theoretically equal the ground acceleration and displacement, respectively; this accounts for the slope that connects the 1.4 g and 0.33 g lines. The corresponding line at the low frequency side is off the graph to the left.

## APPENDIX C—GROUND MOTION DATA

In studying the dependence of peak ground acceleration upon magnitude and distance to the causative fault, the strong-motion literature was critically reviewed in an effort to compile data for which distances to the fault are most reliable, that is, most accurately determined. By restricting the determination to use of only the most reliable data and further to data from a single event, a  $r^{-1.5}$  to  $r^{-2.0}$  dependence of acceleration upon distance is clearly observed for distances as small as 10 km for magnitude 5, 20 km for magnitude 6, and less than 40 km for magnitude 7 (fig. 3). The importance of restricting the data set in determining the near-fault dependence of acceleration upon distance is graphically demonstrated in figure 4, where the scatter in the entire data set is about an order of magnitude greater than the scatter for a single earthquake in figure 3. Because of the  $r^{-1.5}$  to  $r^{-2.0}$  attenuation of acceleration, the

location of the inferred fault is particularly critical at small distances where the data are few.

The data plotted in figure 3 are summarized in table 4. The tabulated acceleration value is the larger of the peak values obtained from the two horizontal accelerograms. Distance is measured to the closest point on the slipped surface of the fault. Except for the Imperial Valley, Hebgen Lake, and Puget Sound earthquakes, the slipped surface is inferred from the spatial distribution of aftershocks located with data from seismographs operated in most cases in the immediate vicinity of the aftershock area. The distance for the Imperial Valley shock is the closest distance to the surface breakage along the Imperial fault. For the Hebgen Lake and Puget Sound shocks, distances to the slipped surface are equated respectively to epicentral distance of the main shock and to hypocentral distance (assuming a minimal focal depth of 45 km). The uncertainties in the distances are given in the last column of table 4.

Table 4.—Peak ground acceleration data for which distances to the causative fault are most accurately known.

DATE YR MO DA	EARTHQUAKE	MAG	STATION	ACC G	DIST KM	UNCER KM
MAGNITUDE 5.0-5.9						
57 03 22	DALY CITY, CALIFORNIA	5.3	S.F., GOLDEN GATE PARK	.13	8.	2-5
			S.F., STATE BLDG.	.11	12.	
			S.F., ALEXANDER BLDG.	.056	14.	
			S.F., SO. PACIFIC BLDG.	.049	14.	
			OAKLAND	.048	24.	
			SAN JOSE	.007	58.	
66 06 28	PARKFIELD, CALIFORNIA	5.5	CHOLAME-SHANDON 2	.52	0.08	0.5
			CHOLAME-SHANDON 5	.48	5.5	
			CHOLAME-SHANDON 8	.28	9.6	
			TEMBLOR	.42	10.6	
			CHOLAME-SHANDON 12	.074	14.9	
			SAN LUIS OBISPO	.019	59.	
			TAFT	.009	101.	
			BUENA VISTA	.007	107.	
			CACHUMA DAM	.003	132.	
			HOLLISTER	.003	137.	
			SANTA BARBARA	.005	154.	
CASTAIC	.005	199.				
UCLA	.001	254.				
			PASADENA	.001	265.	
67 06 21	FAIRBANKS, ALASKA	5.4	COLLEGE	.06	15.	2-5

Table 4.—Peak ground acceleration data for which distances to the causative fault are most accurately known—Continued

DATE YR MO DA	EARTHQUAKE	MAG	STATION	ACC G	DIST KM	UNCER KM
70 09 12	LYTLE CK., CALIFORNIA	5.4	WRIGHTWOOD	.195	15.	2-5
			CEDAR SPRINGS, RANCH	.087	18.	
			CEDAR SPRINGS, DAM	.072	18.	
			DEVILS CANYON	.193	19.	
			SAN BERNARDINO	.125	28.	
			COLTON	.049	29.	
			PUDDINGSTONE DAM	.022	32.	
			LOMA LINDA	.068	34.	
			SANTA ANITA DAM	.057	46.	
MAGNITUDE 6.0-6.9						
40 05 19	IMPERIAL VALLEY, CALIF.	6.4	EL CENTRO	.36	10.	2-5
68 04 09	BORREGO MTN., CALIF.	6.5	EL CENTRO	.12	45.	2
			SAN DIEGO	.030	105.	
			PERRIS RESERVOIR	.018	105.	
			SAN ONOFRE	.041	122.	
			COLTON	.023	130.	
			SAN BERNARDINO	.018	132.	
			DEVILS CANYON	.011	141.	
			CEDAR SPRINGS	.006	147.	
			SANTA ANA	.014	157.	
			SAN DIMAS	.017	168.	
			LONG BEACH, UTIL. BLDG.	.005	187.	
			LONG BEACH, S. CAL. ED.	.008	187.	
			SANTA ANITA RES.	.004	190.	
			VERNON	.011	196.	
			PASADENA, FAC. CLUB	.009	197.	
			PASADENA, SEISMO. LAB.	.007	200.	
			L.A., SUBWAY TERM.	.008	203.	
			L.A., EDISON	.010	203.	
			PEARBLOSSOM	.006	203.	
			WESTWOOD	.006	208.	
			GLENDALE	.024	208.	
			HOLLYWOOD STOR. PE LOT	.007	211.	
			PACOIMA DAM	.009	229.	
			FAIRMONT RESERVOIR	.003	249.	
			LAKE HUGHES #1	.009	253.	
			DAVIS DAM	.003	259.	
			CASTAIC	.008	262.	
			GORMAN	.013	281.	
			PORT HUENEME	.003	288.	
			SANTA BARBARA	.002	341.	
			BAKERSFIELD	.003	342.	
			TAFT	.002	359.	
71 02 09	SAN FERNANDO, CALIF.	6.6	PACOIMA DAM	1.24	3.	2
			L.A., GRIFFITH PARK	.18	16.	
			PASADENA, SEISMO. LAB.	.19	17.	
			SANTA ANITA DAM	.24	25.	
			LAKE HUGHES #12	.37	26.	
			LAKE HUGHES #9	.16	29.	
			TEJON	.03	70.	

Table 4.—Peak ground acceleration data for which distances to the causative fault are most accurately known—Continued

DATE	EARTHQUAKE	MAG	STATION	ACC	DIST	UNCER
YR MO DA				G	KM	KM
71 02 09	SAN FERNANDO (CONTINUED)		SANTA FELICIA DAM	.24+	29.	
			LAKE HUGHES #4	.19	30.	
			CASTAIC	.39	30.	
			LAKE HUGHES #1	.17	32.	
			PALMDALE	.13	35.	
			FAIRMONT RESERVOIR	.10	35.	
			PEARBLOSSOM	.15	43.	
			PUDDINGSTONE DAM	.09	48.	
			PALOS VERDES ESTATES	.04	52.	
			OSD PUMP PLANT	.05	54.	
			LONG BEACH TERM.	.03	58.	
			WRIGHTWOOD	.05	61.	
			PORT HUENEME	.03	71.	
			GRAPEVINE	.07	73.	
			WHEELER RIDGE	.03	88.	
			CEDAR SPRINGS RANCH	.02	94.	
			CEDAR SPRINGS DAM	.03	94.	
			COLTON	.04	97.	
			SAN JUAN CAPISTRANO	.04	102.	
			MARICOPA ARRAY	.01	120.	
			BUENA VISTA	.01	122.	
			SAN ONOFRE	.02	128.	
			TAFT	.02	130.	
			HEMET	.05	142.	
			ANZA	.04	176.	
			SHANDON ARRAY	.01	228.	
MAGNITUDE 7.0-7.9						
49 04 13	PUGET SOUND, WASH.	7.1	OLYMPIA	.31	48.	+10-25
			SEATTLE	.074	69.	+
52 07 21	KERN COUNTY, CALIF.	7.7	TAFT	.20	42.	2-5
			SANTA BARBARA	.14	85.	
			HOLLYWOOD STORAGE, BSMT	.059	107.	
			HOLLYWOOD STORAGE, LOT	.064	107.	
			PASADENA	.055	109.	
			WESTWOOD	.022	110.	
			L.A. SUBWAY TERM.	.032	115.	
			L.A. OCCIDENTAL LIFE	.026	117.	
			VERNON	.037	122.	
			LONG BEACH	.016	145.	
			SAN LUIS OBISPO	.014	148.	
			COLTON	.014	156.	
			BISHOP	.018	224.	
			SAN DIEGO	.005	282.	
			HOLLISTER	.010	293.	
			HAWTHORNE	.004	359.	
			EL CENTRO	.004	370.	
			OAKLAND	.001	407.	
			S.F. SO. PACIFIC BLDG.	.004	425.	
59 08 18	HEBGEN LAKE, MONT.	7.1	BOZEMAN	.068	95.	5-15
			BUTTE	.050	175.	
			HELENA	.022	217.	
			HUNGRY HORSE DAM	.002	454.	

Figures 4 and 6 provide comparison of the better acceleration data for magnitudes 5 and 6, respectively, with acceleration data for which distances to the fault are less well known. The figures include accelerations recorded within 100 km of the fault or epicenter for shocks that provided one or more accelerograms within 32 km. Table 5 summarizes the data, which were obtained from several sources, including the annual issues of "United States Earthquakes." The tabulated acceleration is the larger of the two peak horizontal values. The tabulated distance is the closest distance to the slipped fault, if determinable, or epicentral distance. The uncertainty in distance is indicated by the letter A, B or C, representing estimated uncertainties of less than 2 km, 2-5 km, and 5-25 km, respectively.

Table 5 also summarizes the velocity, displacement and duration data plotted in figures 8, 9 and 10, respectively. Figure 8 illustrates the dependence of peak horizontal ground velocity upon magnitude and distance. The velocity data,

derived by integration of accelerograms, were obtained primarily from three sources (Hudson and others 1971; Wiggins, 1964; and Ambroseys, 1969). The tabulated velocity is the larger of the two peak horizontal values.

The displacement data in figure 9 are derived from displacement records obtained either directly from 10-second displacement meters or analytically by double integration of accelerograms. Data from the 10-second displacement meters are taken from the annual issues of "United States Earthquakes." Displacements obtained from twice-integrated accelerograms are primarily from Hudson, Brady, Trifunac, and Vijayaraghavan (1971) and correspond to ground motion from which spectral components with periods longer than about 15 Hz are removed. The tabulated displacement is the larger of the two peak horizontal values.

The 0.05 g durations plotted in figure 10 were measured from published accelerograms. The larger of the two horizontal durations is tabulated.

Table 5.—Strong motion data plotted on graphs showing peak horizontal acceleration, velocity, and dynamic displacement and duration of shaking as a function of distance to slipped fault (or epicentral distance)

DATE YR MO DA	EARTHQUAKE	MAG	STATION	DISTANCE KM *		ACC G	VEL CM/SEC	DISP CM **	DUR SEC
MAGNITUDE 5.0-5.9									
33 10 02	LONG BEACH	5.4	VERNON	14	C	.115			2.0
			LONG BEACH	15		.077			1.0
			L A SUB TERM	19		.082+		.8 D	0.0+
			WESTWOOD	24		.009+			
			HOLLYWOOD STOR	27		.033+			
			PASADENA	30		.005+		.2 D	
34 07 06	N CALIF COAST	5.7	EUREKA	149	C			.9 D	
35 01 02	C MENDOCINO	5.8	EUREKA	117	C			.1+D	
35 11 28	HELENA, MONT	5.2	HELENA	8	C	.082	3.9		
37 02 07	C MENDOCINO	5.8	FERNDALE	84	C		3.8	.6+D	
38 5 31	SANTA ANA MT	5.5	COLTON	47	C			.2+D	
			L A SUB TERM	78				.1-D	
38 09 12	C MENDOCINO	5.5	FERNDALE	51	C		6.1		
40 05 19	IMPERIAL VAL	5.2	EL CENTRO	16	C	.077			0.5
40 12 20	C MENDOCINO	5.5	FERNDALE	91	C		4.4		
			EUREKA	103				.5 D	
41 07 01	SANTA BARBARA	5.9	SANTA BARBARA	14	C	.175+	20.3		
			L A SUB TERM	127				.2 D	

Table 5.—Strong motion data plotted on graphs showing peak horizontal acceleration, velocity, and dynamic displacement and duration of shaking as a function of distance to slipped fault (or epicentral distance)—Continued

DATE		EARTHQUAKE	MAG	STATION	DISTANCE		ACC G	VEL CM/SEC	DISP CM **	DUR SEC	
YR	MO DA				KM	*					
41	10 21	GARDENA	5.	VERNON	13	C	.017				
				L A CHAMB COM	14		.018				
				L A SUB TERM	16		.009			.3 D	
				L A EDISON	16		.009				
				LONG BEACH	17		.033				
				WESTWOOD	20		.005				
				HOLLYWOOD STOR	21		.006				
41	11 14	TORRANCE	5.5	LONG BEACH	15	C	.050				
				VERNON	19		.019				
				L A CHAMB COMM	20		.014				
				L A SUB TERM	22		.009			.4 D	
				L A EDISON	22		.009				
				WESTWOOD	25		.009				
				HOLLYWOOD STOR	25		.008				
43	08 29	BIG BEAR LAKE	5.5	COLTON	39	C			.3 D		
45	08 15	BORREGO VAL	5.7	EL CENTRO	68	C		1.0			
47	05 27	C MENDOCINO	5.2	FERNDAL	30	C			.5+D		
47	09 23	C MENDOCINO	5.3	FERNDAL	77	C			.1 D		
48	08 18	C MENDOCINO	5.0	FERNDAL	26	C			.1-D		
49	03 09	HOLLISTER	5.2	HOLLISTER	21	C	.20	7.6		6.5	
				SAN JOSE	48		.004				
				S F SO PACIFIC	119						.1-D
50	07 29	CALIPATRIA	5.5	EL CENTRO	35	C		1.0			
51	01 24	CALIPATRIA	5.6	EL CENTRO	30	C	.033	4.3			
51	07 29	MULBERRY	5.0	HOLLISTER	34	C		1.1			
51	12 25	SAN CLEMENTE I	5.9	L A SUB TERM	137	C			.3 D		
52	09 22	PETROLIA	5.2	FERNDAL	38	C		6.4	1.9 D		
53	06 14	IMPERIAL	5.5	EL CENTRO	12	C	.045	6.9			
54	01 27	TEHACHAPI	5.0	ARVIN	19	C	.045				
54	02 01	BAJA CALIF	5.6	EL CENTRO	60	C		1.1			
54	04 25	WATSONVILLE	5.3	HOLLISTER	20	C	.059	3.9		0.5	
55	08 08	S W NEVADA	5.2	HAWTHORNE	24	C	.010				
55	09 04	SAN JOSE	5.5	SAN JOSE	10	C	.13	10.8	2.8 A	1.5	
				OAKLAND	64		.007				
				HOLLISTER	67		.048				4.5
				S F ALEXANDER	71		.008				
				S F SO PACIFIC	73		.011				
55	10 23	WALNUT CREEK	5.4	SUISUN BAY BRG	8	C	.12				
				BERKELEY	21		.020				
				OAKLAND	29		.023				
				S F SO PACIFIC	36		.022				
				S F STATE	42		.023				

Table 5.—Strong motion data plotted on graphs showing peak horizontal acceleration, velocity, and dynamic displacement and duration of shaking as a function of distance to slipped fault (or epicentral distance)—Continued

DATE	EARTHQUAKE	MAG	STATION	DISTANCE	ACC	VEL	DISP	DUR
YR MO DA				KM *	G	CM/SEC	CM **	SEC
55 12 17	BRAWLEY	5.4	EL CENTRO	22 C	.083+	5.1		1.0+
57 03 22	DALY CITY	5.3	S F GOLDN GATE	8 B	.129	4.9	2.3 A	1.5
			S F STATE	12	.105	5.1	1.1 A	1.0
			S F STATE	12			1.1 D	
			S F ALEXANDER	14	.056	2.9	1.3 A	0.0+
			S F SO PACIFIC	14	.049	5.0	1.4 A	0.0
			OAKLAND	24	.048	2.0	1.5 A	0.0
			SAN JOSE	58	.007			
57 04 25	CALIPATRIA	5.2	EL CENTRO	51 C			.6 D	
57 04 25	CALIPATRIA	5.1	EL CENTRO	51 C			.4 D	
60 01 19	HOLLISTER	5.0	HOLLISTER	8 C	.064			3.0
61 04 09	HOLLISTER	5.6	HOLLISTER	20 C	.193	17.1	3.8 A	5.5
62 08 30	LOGAN, UTAH	5.7	LOGAN	7 C	.12			2.5
63 02 28	FORT TEJON	5.0	WHEELER RIDGE	8 C	.058			
66 06 28	PARKFIELD	5.5	CHOLAME-SHAN 2	0.1A	.52	72.2	22.3 A	12.0
			CHOLAME-SHAN 5	5.5	.48	27.3	8.4 A	8.5
			CHOLAME-SHAN 8	9.6	.28	12.6	6.7 A	9.0
			TEMBLOR	10.6	.42	21.0	8.1 A	5.5
			CHOLAME-SHAN12	14.9	.074	6.5	7.1 A	5.0
			SAN LUIS OBISP	59	.019			
67 06 21	FAIRBANKS, AK	5.4	COLLEGE	15 B	.06			
67 12 10	N CALIF COAST	5.8	FERNDALE	32 C	.10			1.0
70 09 12	LYTLE CREEK	5.4	WRIGHTWOOD	15 B	.195			2.5
			CEDAR SPR RCH	18	.087			
			CEDAR SPR DAM	18	.072			
			DEVILS CANYON	19	.193			4.5
			SAN BERNARDINO	28	.125			1.0
			COLTON	29	.049			
			PUDDINGSTONE D	32	.022			
			LOMA LINDA	34	.068			
			SANTA ANITA D	46	.057			
MAGNITUDE 6.0-6.9								
33 03 11	LONG BEACH	6.3	LONG BEACH	5 C	.23+			7.0+
			VERNON	20	.17	20.0		7.5
			L A SUB TERM	25	.06			5.0
33 06 25	W NEVADA	6.1	S F SD PACIFIC	302 C			.2+D	
34 06 07	PARKFIELD	6.	PASADENA	298			.2 D	
34 12 30	MEXICALI, MEX	6.5	EL CENTRO	64 C		15.5		
			L A SUB TERM	328			.3 D	
35 10 31	HELENA	6.0	HELENA	7.5C	.16	16.8		1.5
37 03 25	COAHUILA VAL	6.	COLTON	94 C			.2 D	
			PASADENA	160			.1 D	
			L A SUB TERM	167			.3 D	

Table 5.—Strong motion data plotted on graphs showing peak horizontal acceleration, velocity, and dynamic displacement and duration of shaking as a function of distance to slipped fault (or epicentral distance)—Continued

DATE YR MO DA	EARTHQUAKE	MAG	STATION	DISTANCE KM *	ACC G	VEL CM/SEC	DISP CM **	DUR SEC
40 05 19	IMPERIAL VAL	6.4	EL CENTRO L A SUB TERM	10 B 300	.36	36.9	19.8 A .9 D	
41 02 09	C MENDOCINO	6.0	FERNDAL EUREKA	89 C 107		3.5	.8 D	
41 05 13	C MENDOCINO	6.	FERNDAL	211 C		0.9		
41 10 03	C MENDOCINO	6.4	FERNDAL EUREKA	67 C 82		5.6	.9 D	
42 10 21	BORREGO VAL	6.5	EL CENTRO COLTON L A SUB TERM	48 C 172 241		6.0	.4 D .8 D	
46 03 15	WALKER PASS	6.3	PASADENA L A SUB TERM	177 C 188			.5+D .4 D	
47 04 10	MANIX	6.2	COLTON	123 C			.4 D	
48 12 04	DESERT HOT SPG	6.5	COLTON PASADENA L A SUB TERM	93 C 167 178			.3 D .4 D .8 D	
51 10 08	C MENDOCINO	6.0	FERNDAL FERNDAL	41 C 41		7.4	2.7 A 1.0 D	
54 03 19	SANTA ROSA MTS	6.2	EL CENTRO	80 C		2.5		
54 11 12	BAJA CALIF	6.3	EL CENTRO	150 C		3.8		
54 12 21	HUMBOLDT CO	6.5	EUREKA FERNDAL FERNDAL	20 C 40 40	.29 .21	31.6 35.6	14.1 A 14.2 A 6.4+D	8.0 11.0
56 02 09	BAJA CALIF	6.8	EL CENTRO EL CENTRO	122 C 122		7.0	4.1 A 4.2 D	
56 02 09	BAJA CALIF	6.1	EL CENTRO EL CENTRO	122 C 122		2.7	2.3 A 1.0+D	
56 10 11	C MENDOCINO	6.0	FERNDAL	121 C		1.3		
65 04 29	SEATTLE, WASH	6.5	SEATTLE OLYMPIA	63 C 84		17.0 16.0		
67 12 11	KOYNA, INDIA	6.3	KOYNA	5 C	.62	25.3		
68 04 09	BORREGO MTN	6.5	EL CENTRO SAN DIEGO	45 B 105		25.8 6.1	12.2 A 4.4 A	3.0

Table 5.—Strong motion data plotted on graphs showing peak horizontal acceleration, velocity, and dynamic displacement and duration of shaking as a function of distance to slipped fault (or epicentral distance)—Continued

DATE YR MO DA	EARTHQUAKE	MAG	STATION	DISTANCE KM *	ACC G	VEL CM/SEC	DISP CM **	DUR SEC
71 02 09	SAN FERNANDO	6.6	PACOIMA DAM	3 B	1.24	115.	43. A	13.0
			L A GRIFFITH	16	.18			10.0
			PASADENA, SEIS	17	.19			7.0
			SANTA ANITA D	25	.24			11.5
			LAKE HUGHES 12	26	.37			14.0+
			LAKE HUGHES 9	29	.16			4.5+
			SANTA FELICIA	29	.24			6.5+
			LAKE HUGHES 4	30	.19			4.0
			CASTAIC	30	.39			18.0+
			LAKE HUGHES 1	32	.17			9.0
			PALMDALE	35	.13			
			FAIRMONT RES	35	.10			
			PEARBLOSSOM	43	.15			
			PUDDINGSTONE D	48	.09			
			PALOS VERDES	52	.04			
			OSO PUMP PLANT	54	.05			
			LONG BEACH TRM	58	.03			
			WRIGHTWOOD	61	.05			
			TEJON	70	.03			
			PORT HUENEME	71	.03			
			GRAPEVINE	73	.07			
			WHEELER RIDGE	88	.03			
			CEDAR SPR RCH	94	.02			
			CEDAR SPR DAM	94	.03			
			COLTON	97	.04			
MAGNITUDE 7.0-7.9								
40 05 19	IMPERIAL VAL	7.1	EL CENTRO	10.8				29.5
49 04 13	PUGET SND, WASH	7.1	OLYMPIA	48+ C		21.0		23.0
			SEATTLE	69+				15.0
52 07 21	KERN COUNTY	7.7	TAFT	42 B		17.7	9.2 A	19.5
			SANTA BARBARA	85		19.3	5.8 A	10.5
			HOLLYWOOD BSMT	107		9.4	5.9 A	
			HOLLYWOOD LOT	107		8.9	6.4 A	
			PASADENA	109		9.1	2.9 A	
			PASADENA	109			4.5 D	
			L A SUB TERM	115			5.7 D	
			COLTON	156			2.6 D	
54 12 16	FALLON, NEV	7.0	S F SO PACIFIC	404			1.4 D	
			L A SUB TERM	584			3.6 D	

NOTES:

\* UNCERTAINTY IN DISTANCE: A=LESS THAN 2 KM  
 B=2 TO 5 KM  
 C=5 TO POSSIBLY 25 KM

\*\* SOURCE OF DISPLACEMENT DATA: A=DOUBLE INTEGRATION OF ACCELEROGRAM  
 D=10-SEC DISPLACEMENT METER

